Computer simulation of hypervelocity impacts

Cite as: AIP Conference Proceedings **2504**, 030031 (2023); https://doi.org/10.1063/5.0132803
Published Online: 16 February 2023

Igor Lomonosov, Vadim Kim and Afanasii Ostrik

Computer Simulation of Hypervelocity Impacts

Igor Lomonosov,[a] Vadim Kim,[b] and Afanasii Ostrik[c]

Institute of Problems of Chemical Physics of the Russian Academy of Sciences
Ac. Semenov avenue 1, Chernogolovka, Moscow region, 142432 Russian Federation

[a] *Corresponding author: ivl143@ficp.ac.ru*
[b] *Electronic mail: kim@ficp.ac.ru*
[c] *Electronic mail: ostrik@ficp.ac.ru*

Abstract. This research presents a modification of "finite–size particle in cell" method developed for numerical modeling of processes at high energy density. It uses the Lagrangian–Eulerian representation of media which allows one to match contact and free surfaces and to calculate flows with strong deformations. Efficient models of thermodynamic properties, elastic–plastic deformation and fragmentation have been employed in the gas dynamic code adapted for parallel computations. 3D and 2D numerical modeling of plates penetrations by impactors of different geometry has been done in a wide range of velocities. The influence of used materials properties models on numerical results has been investigated.

INTRODUCTION

The problem of hypervelocity impact is of fundamental interest and has numerous practical applications, e.g. protection for space vehicles [1], collisions of asteroids with planets [2] and others. Experimental investigations of hypervelocity impacts are very complicated and it is necessary to use the numerical modeling for better understanding of details of the processes and of the gas dynamic flow.

Nowadays numerical methods have been developed to solve multi–dimension non–stationary gas dynamic problems, which proved efficient for selected tasks. Methods based on representation of continuous media as an aggregation of discrete particles [1, 3, 4, 5, 6] are used in modeling of multi–phase flows characterized by strong deformations and by change of topological structure of computational area. In this approach each computational particle posses an information about well–defined final volume of specific material under conditions formed in the process of moving. Simple and natural methods allowing one to calculate contact boundaries, formation of new phases and different types of matter failuring, including discontinuities of medium, are also advantages in comparison with other schemes.

The current state of the problem of a theoretical description of thermodynamic properties of matter at high pressures, high temperatures is given in a set of publications [1, 7, 8, 9, 10]. The range of applicability of modern theories is local and rigorously speaking, none of them allows to provide for a correct theoretical calculation of thermodynamic properties of matter over the entire phase plane from the cold crystal to liquid and hot plasmas. In this case experimental data at high pressures, high temperatures are of peculiar significance, because they serve as reference points for theories and semiempirical models [9]. Details of investigations of mechanic properties of matter, such as experimental methods and corresponding theoretical models, are given in books [9, 11].

In this paper we present a modification of "finite–size particle in cell" method [12] for parallel gas–dynamics applications. 3D numerical modeling of hypervelocity impacts of different shape impactors with thin plate targets has been done. We investigated processes of impact, penetration, debris cloud and hole formation. The density distribution and the shape of debris cloud were controlled, as well as the hole diameter.

NUMERICAL ALGORITHM

The proposed algorithm uses on Eulerian step an implicit conditionally–stable (even at zero artificial viscosity) conservative finite–difference scheme. The matter transport is modeling on Lagrangian step by movement of finite–size particles. A special attention is paid to numerical procedures of particle's packing and repacking, their splitting and merging. As a result, this method leads to obtaining monotonic profiles of the matter parameters and to tracking efficiently body interfaces. Different code modifications accounting for models of multi–component and heterogenous media can be naturally developed with the use of the particle approach.

A traditional two–step PIC–method scheme is employed in the code to integrate the conservation equations in time. As a first step, no convective flows are supposed, so movement and energy equations are written in cartesian coordi-

Actual Problems of Continuum Mechanics: Experiment, Theory, and Applications
AIP Conf. Proc. 2504, 030031-1–030031-6; https://doi.org/10.1063/5.0132803
Published by AIP Publishing. 978-0-7354-4406-5/$30.00

nates in form $\frac{\partial \rho \vec{u}}{\partial t} = \nabla \widehat{P}, \rho \frac{\partial e}{\partial t} = \nabla(\widehat{P}\vec{u})$, where $\widehat{P} = \begin{pmatrix} \sigma_{xx} - p & \sigma_{xy} & \sigma_{xz} \\ \sigma_{yx} & \sigma_{yy} - p & \sigma_{yz} \\ \sigma_{zx} & \sigma_{zy} & \sigma_{zz} - p \end{pmatrix}$, p, σ_{ij}, ρ, $\vec{u}$, e — stress tensor, pressure, deviatric stress tensor, density, velocity vector, specific internal energy at given spatial point, correspondingly, t— time.

The continuity equation is calculated automatically for the moment when the medium is motionless. For finite–difference presentation of this system let's refer thermodynamic derivatives (density, pressure, internal energy) to cell centers, while kinematic (components of velocity vector) — to nodes of computational grid. So approximations of movement for x–velocity component u (for v and w components—analogues) and energy equations are [**?**]

$$\frac{u_{ijk}^{n+1} - u_{ijk}^{n}}{\Delta t} = -\frac{\Delta y \Delta z}{4M_{ijk}} \Big[(p+q^x)_{ijk}^{n} - (p+q^x)_{i-1\,jk}^{n} + (p+q^x)_{ij-1k}^{n} - (p+q^x)_{i-1\,j-1k}^{n} + (p+q^x)_{ijk-1}^{n} - (p+q^x)_{i-1\,jk-1}^{n} + (p+q^x)_{ij-1k-1}^{n} - (p+q^x)_{i-1\,j-1k-1}^{n} \Big],$$

$$\begin{aligned} \frac{e_{ijk}^{n+1} - e_{ijk}^{n}}{\Delta t} = -\frac{1}{4m_{ijk}} \Big[& (u_{i+1jk}^{n+\frac{1}{2}} - u_{ijk}^{n+\frac{1}{2}} + u_{i+1j+1k}^{n+\frac{1}{2}} - u_{ij+1k}^{n+\frac{1}{2}} + u_{i+1jk+1}^{n+\frac{1}{2}} - u_{ijk+1}^{n+\frac{1}{2}} + \\ & + u_{i+1j+1k+1}^{n+\frac{1}{2}} - u_{ij+1k+1}^{n+\frac{1}{2}})(p+q^x)_{ijk}^{n} \Delta y \Delta z + (v_{ij+1k}^{n+\frac{1}{2}} - v_{ijk}^{n+\frac{1}{2}} + v_{i+1j+1k}^{n+\frac{1}{2}} - v_{i+1jk}^{n+\frac{1}{2}} + \\ & + v_{ij+1k+1}^{n+\frac{1}{2}} - v_{ijk+1}^{n+\frac{1}{2}} + v_{i+1j+1k+1}^{n+\frac{1}{2}} - v_{i+1jk+1}^{n+\frac{1}{2}})(p+q^y)_{ijk}^{n} \Delta x \Delta z + (w_{ijk+1}^{n+\frac{1}{2}} - w_{ijk}^{n+\frac{1}{2}} + \\ & + w_{i+1jk+1}^{n+\frac{1}{2}} - w_{i+1jk}^{n+\frac{1}{2}} + w_{ij+1k+1}^{n+\frac{1}{2}} - w_{ij+1k}^{n+\frac{1}{2}} + w_{i+1j+1k+1}^{n+\frac{1}{2}} - w_{i+1j+1k}^{n+\frac{1}{2}})(p+q^z)_{ijk}^{n} \Delta x \Delta y \Big], \end{aligned}$$

where $\Delta t, \Delta x, \Delta y, \Delta z$—— time and spatial resolutions, u, v, w—components of velocity vector, p—pressure, q^x, q^y, q^z—components of artificial viscosity, m_{ijk}—mass in cell, M_{ijk}—averaged mass in ijk node. Top indexes correspond to temporal variables, bottom ones correspond nodes of computational grid. Top fractional indexes indicate averaged values on n and $n+1$ temporal steps. An artificial viscosity is given as

$$\begin{aligned} q_{ijk}^{x} = \frac{1}{4} k \cdot \rho_{ijk}^{n} \cdot c_{ijk}^{n} \Big[& u_{i+1jk}^{n} - u_{ijk}^{n} + u_{i+1j+1k}^{n} - u_{ij+1k}^{n} + \\ & + u_{i+1jk+1}^{n} - u_{ijk+1}^{n} + u_{i+1j+1k+1}^{n} - u_{ij+1k+1}^{n} \Big], \end{aligned}$$

where k characterizes the shock front smoothing. The value of k equals 0 when the condition is satisfied

$$\begin{aligned} \Big[& u_{i+1jk}^{n} - u_{ijk}^{n} + u_{i+1j+1k}^{n} - u_{ij+1k}^{n} + \\ & + u_{i+1jk+1}^{n} - u_{ijk+1}^{n} + u_{i+1j+1k+1}^{n} - u_{ij+1k+1}^{n} \Big] > 0. \end{aligned}$$

Here c_{ijk}^{n} is a sound speed in a cell.

The computation of convective transfer through boundaries of Eulerian cells is carrying out on Lagrangian step. It has following features: the continuous medium is modeled by system of finite–size cuboids; mass, pulse and internal energy of each particle are uniformly distributed in its volume; all particles move forward through grid without rotation; particle position is completely defined by coordinates of mass center and linear sizes; particle mass remains constant during its move.

A new intermediate distribution of velocities and internal energy occurs after the Eulerian step. The packing of particles, i.e. transfer of medium characteristics from Eulerian grid to the system of particles, is carrying out on the preliminary step. The flow parameters in the particle are identical to the one's in the cell when "pure" cell includes particles of only one material. The other case corresponds to "mixed" cell including particles of two or more materials. In this situation internal energy in particles and their new densities are determined from condition of equality of pressure and temperature inside the cell, as it is done for the elementary cell of heterogeneous material [13]. Then a new position of particles resulting from their move is computed: $x_{i_N}^{n+1} = x_{i_N}^{n} + u_{i_N} \Delta t$. These data are used to transfer all medium characteristics from particles to Eulerian grid. The procedure of splitting particles by Eulerian grid with further merging of particles of the same material inside one cell is used. It helps to conserve the uniform regular structure of particles, i.e. the Lagrangian grid with nodes in particle's centers. Splitting and merging procedures

prevent from occurrence of hollow cells in a region of strong expansion and smooth enough unphysical oscillations related with discrete treatment of mass flows. In addition, as the number of computational particles in each period of time is proportional to number of occupied grid cells, rather then the maximum dimension of computational area, the high demands to operative memory decrease significantly.

The procedure of particle's splitting is based on the geometry. If a particle occupies more then one Eulerian cell, it is splitted along coordinate axes of computational grid on corresponding amount of fragments. Here all physical parameters of obtained particles (density, internal energy, velocity components, body marker, and others) are equal to those of the original particle. Only new coordinates of particle's centers and linear sizes are recalculated. The total volume remains constant in this procedure. The merging procedure is carrying out for pairs of particles. It has following features: conservation of full energy, mass and volume of particles; center of merged particle is the mass center of merging particles, its density is a ratio of total mass of merging particles to their total volume; particle velocity is defined by momentum conservation law; internal energy equals the difference between total energy and kinetic one; size of merged particle is defined by total volume of merging particles and is proportional to dimension of Eulerian cell.

The repacking procedure serves to compute flow parameters in Eulerian grid. Parameters of merged particle coincides with parameters in the center of cell. The total energy is transferred by the particle; the internal energy equals the difference between total energy and kinetic one in "pure" cell. For "mixed" cell the internal energy is averaged using total mass of particles in this cell. New velocity components in the node of Eulerian grid are defined by total averaging of pulse components of particles joined to this node.

The gas dynamic code has been developed on the base of this algorithm. The parallel version uses Single Process—Multiple Data programming model with coarse–grain data decomposition. Message Passing Interface has been used for interprocess communications. Numerical tests of Riemann problem in an ideal gas corresponds to an analytical solution. The shock front smoothed in less then six cells with practically correct position of contact discontinuity.

The productivity of the parallel implementation of the numerical algorithms was examined on several multiprocessor supercomputers including "Lomonosov–2" at Moscow State University. The softest task statement with the simple full computational area coverage with the body particles and with the equal loading of the different CPU-nodes was utilized to exclude balance–loading fluctuations. Profiling results for the different amount of CPU–nodes used are presented on Fig. 1. Computational load per one CPU–node is fixed, so the total computational area grows proportionally to the number of CPU–nodes used. Amount of time required for the interprocess communications (MPI) remains on the same level with the number of used CPU–nodes increased so demonstrating an efficient usage of the parallel algorithms.

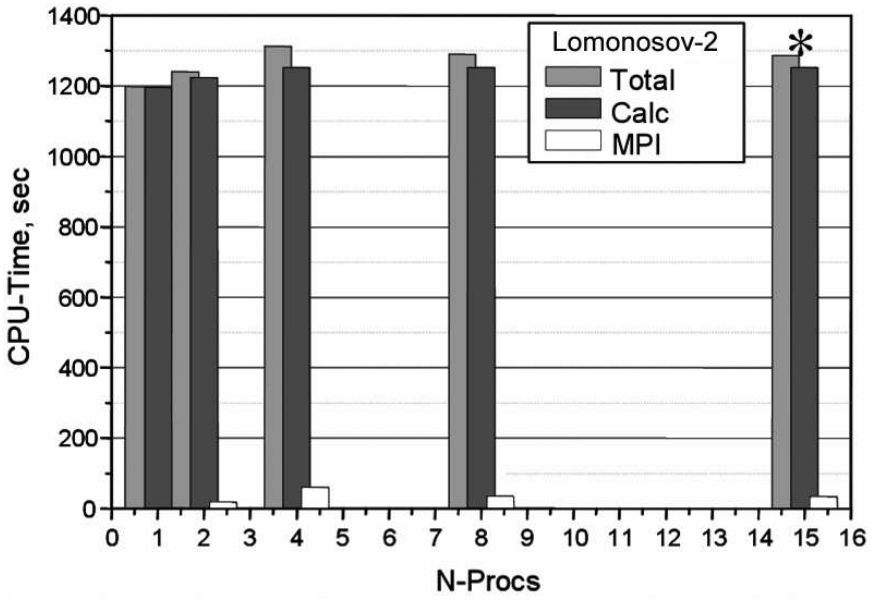

FIGURE 1. Parallel CPU–time profiling results on Lomonosov–2 supercomputer at MSU.

EQUATION OF STATE AND CONSTITUTIVE RELATIONS

The advanced multi–phase EOS [14] fully assigns the free energy thermodynamic potential over entire phase diagram region of practical interest. It accounts for solid, liquid, plasma states as well as two-phase regions of melting and evaporation. The following information at high pressures, high temperatures: measurements of isothermal compressibility in diamond anvil cells, data on sound velocity and density in liquid metals at atmospheric pressure, isobaric–expansion measurements, registrations of shock compressibility for solid and porous samples in incident and reflected shock waves, impedance measurements of a shock compressibility under condition of an underground nuclear explosion, data on isentropic expansion of shocked metals, calculations by Debye–Hueckel and Thomas–Fermi models, evaluations of the critical point were used to construct this EOS.

The ideal plasticity model is used to account for elastic–plastic properties of matter:

$$\frac{d\sigma_{ij}}{dt} = (1+\delta_{ij})G(\varepsilon_{ij} - \frac{1}{3}\delta_{ij}\Delta V),$$

where δ_{ij}—Kroneker delta, ε_{ij}—components of strain tensor, $\Delta V = \varepsilon_{ii}$, G— shear modulus. The yield condition is chosen in von Misses formulation

$$\sigma_{ij} = \begin{cases} \sigma_{ij}, & J < \frac{2}{3}Y_0 \\ \sigma_{ij}\frac{\sqrt{\frac{2}{3}Y_0^2}}{\sqrt{J}}, & J > \frac{2}{3}Y_0 \end{cases}$$

where $J = \sum_{i=1}^{3}\sum_{j=1}^{3}\sigma_{ij}^2 = \sigma_{xx}^2 + \sigma_{yy}^2 + \sigma_{zz}^2 + 2(\sigma_{xy}^2 + \sigma_{xz}^2 + \sigma_{yz}^2)$, Y_0—yield strength.

Spallation effects are described by the fracture model [11]. The material porosity is calculated on each time step as

$$V_p^{n+1} = \sqrt[1-\beta]{(V_p^n)^{1-\beta} + (1-\beta)\frac{\sigma}{\tau\sigma_p}\left(\frac{\sigma_{max}}{\sigma_p}\right)^{\alpha-1}dt},$$

where σ_{max}— maximum mean stress on particle; σ— current mean stress in particle; α, β, τ, σ_p— fitting coefficients. The crack forms when the porosity reaches the critical value, then the porosity is chosen to fit the value of pressure to 0.

RESULTS OF NUMERICAL SIMULATION

The problem of thin plates penetration by impactor of different geometry and impact angle has been investigated. Impact of an iron ball (0.5 mm diameter) at velocity of 4 km/s on a aluminum plate (0.5 mm thickness) with the impact angles of 30 and 60 degrees were simulated using parallel computer code developed.

Results of computer modeling for the impact angles of 60 and 30 degrees are shown on Fig. 2–5. 2D-pressure and density fields distribution at 0.1 μs, 0.25 μs and 0.5 μs for 60 degrees angle are presented on Fig. 2 and Fig. 3 respectively.

Comparing with the analogues results for 30 degrees impact (Fig. 4 and Fig. 5) one can see that sharper angle value leads to more pronounced asymmetry of the crown of splashed target material. For the 30 deg impact part of the target material hits back the rear surface of the target plate. Also the more intensive compression wave is formed in the plate along the direction of impact. Penetration velocity and depth are decreased as it was expected.

While further decreasing the impact angle it is also important to take into account the boundary conditions between iron impactor and aluminum target and slipping of materials. Due to the slipping boundary effects the most of the ball kinetic energy spent on the compression of target material near the front surface area and not on the transverse plate penetration.

As a result the difference of the damaged plate crater sizes for normal and 60 degrees impacts is insignificant: 1.9 and 2.0 mm respectively. For the 30 degrees impact the final target crater diameter is 2.5 mm.

CONCLUSION

Numerical modeling of hypervelocity impacts has been done with new parallel implementation of "finite–size particle in cell" method. The 3D gas dynamic code includes advanced physical models of matter at high energy density.

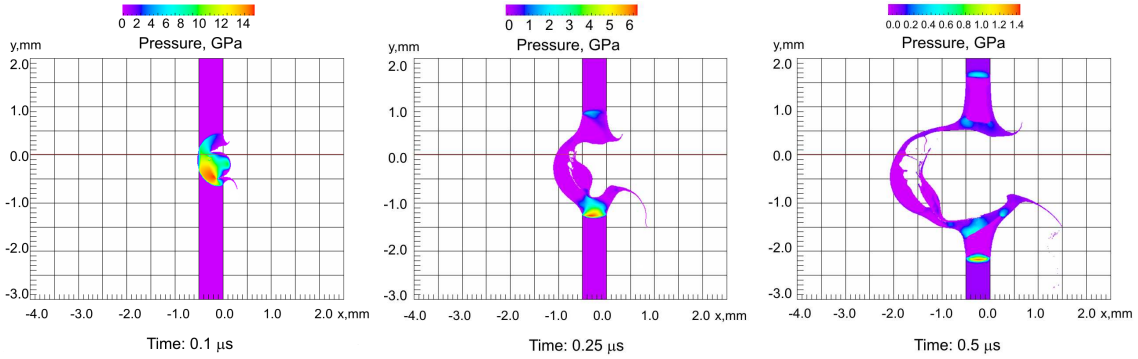

FIGURE 2. 2D-pressure field for 60 degrees impact angle 4 km/s velocity penetration, at 0.1 μs, 0.25 μs and 0.5 μs.

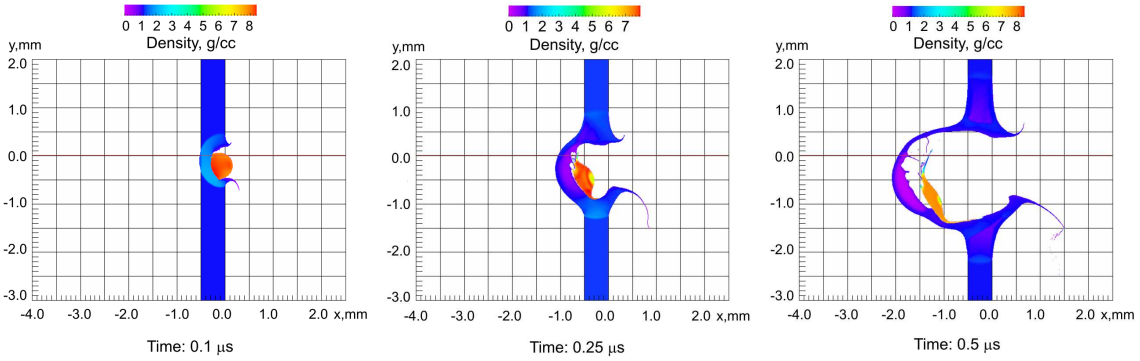

FIGURE 3. 2D-density field for 60 degrees impact angle 4 km/s velocity penetration, at 0.1 μs, 0.25 μs and 0.5 μs.

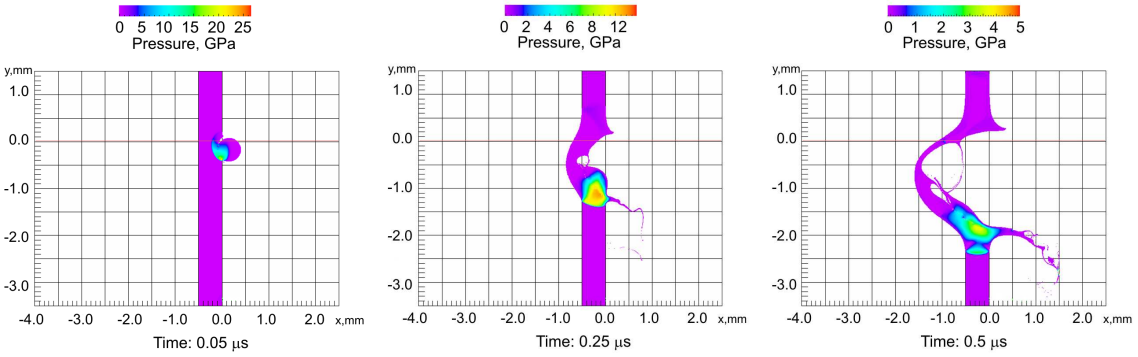

FIGURE 4. 2D-pressure field for 30 degrees impact angle 4 km/s velocity penetration, at 0.05 μs, 0.25 μs and 0.5 μs.

The robust and effective implementation of the parallel data processing algorithms was demonstrated using modern supercomputer facilities. Calculations carried out with the use of different EOS demonstrated the necessity to take into account the effect of evaporating for high values of impact velocity. In the case of moderate impact velocities, an influence of rheological models on results of numerical modeling has been investigated. It was shown that the calculated diameter of the impact crater depends on accounting for elastic–plastic and strength properties.

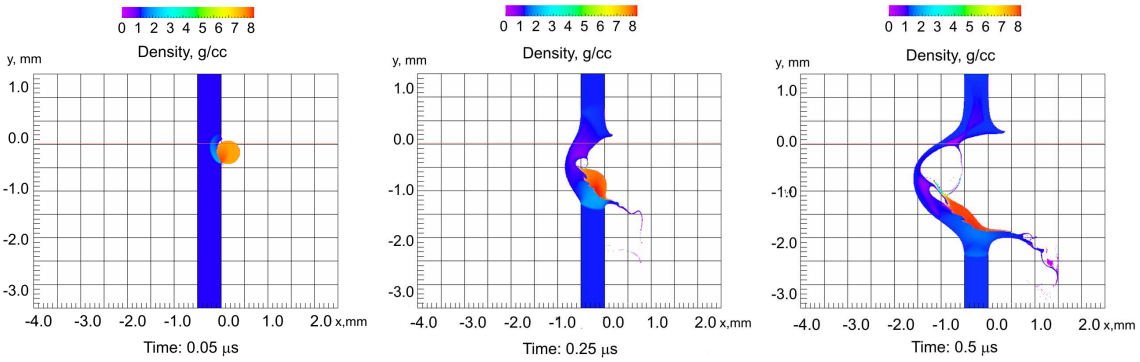

FIGURE 5. 2D-density field for 30 degrees impact angle 4 km/s velocity penetration, at 0.05 μs, 0.25 μs and 0.5 μs.

ACKNOWLEDGMENTS

The research was supported by The Ministry of Science and Higher Education of the Russian Federation (Agreement with Joint Institute for High Temperatures RAS No 075-15-2020-785 dated September 23, 2020).

REFERENCES

1. Fortov VE et al. Thermophysical and gas dynamic problems of meteoroid protection of space vehicle “Vega”. Teplofiz Visokh Temper 1984; 22:964 [in Russian].
2. Gerels T, editor. Hazards due to comets and Asteroids. Univ. of Arizona Press:1994.
3. Harlow FH. The Particle-in-cell Computing Method in Fluid Dynamics. Methods Comput Phys 1964; 3:319.
4. Belotserkovskii OM, Davydov YuM. The Method of Large Particles in Gasdynamics. Moscow: Nauka, 1982 [in Russian].
5. Jentry RA, Martin RE, Daly BJ. An Eulerian Differencing Method for Unsteady compressible Flow Problems. J Comput Phys 1966; 1(1):87-118.
6. Morse RL. Multidimensional plasma simulation by the particle-in-cell method. In: Alder B, Fernback S, Rothenberg M, editors. Methods in Computational Physics: Plasma Physics, volume 9 of Methods in Computational Physics. New York, Academic Press, 1970. p. 213-239.
7. Zeldovich YaB, Raizer YuP. Physics of Shock Waves and High-Temperature Hydrodynamic Phenomena. New York: Academic Press, 1966.
8. Caldirola P, Knoepfel H, editors. Physics of High Energy Density. New York: Academic Press, 1971.
9. Bushman AV, Kanel GI, Ni AL, Fortov VE. Intense Dynamic Loadings of Condensed Matter. London: Taylor-Francis, 1993.
10. Fortov VE, Yakubov IT. Physics of Nonideal Plasmas. London: World. Sci. Publ. Co. PTE. LTD, 1999.
11. Kanel GI, Razorenov SV, Utkin AV, Fortov VE. Shock phenomena in condensed matter. Moscow: “Yanus-K”, 1996. [in Russian]
12. Fortov VE et al. Numerical modeling of hypervelocity impacts. Int J Impact Engng 2006. Vol.33, Issue 12, p.244-253.
13. Ostrik AV. Thermodynamical influence of x-rays on multilayer obstacles. Moscow: NTC “Informtehnika”, 2003. [in Russian]
14. Lomonosov IV. Multi-phase equation of state for aluminum. Laser and Particle beams 2007. Vol.25(04), p.567-584.